Article

Journal of Chitin and Chitosan Science
Vol. 2, 46–54, 2014
www.aspbs.com/jcc

Application of Chitosan Coating on Alginate Beads for Cryopreservation Uses

A. S. Teixeira[1, 2, *], L. Deladino[2], C. F. Fernandes[1, 3], M. Martino[2], and A. D. Molina-García[1]

[1] *Instituto de Ciencia y Tecnología de Alimentos y Nutrición, ICTAN-CSIC, José Antonio Novais 10, 28040 Madrid, Spain*
[2] *Centro de Investigación y Desarrollo en Criotecnología de los Alimentos (CIDCA), CONICET, Fac. Cs. Exactas (UNLP), 47 y 116, La Plata, 1900, Argentina*
[3] *Escola Superior de Biotecnologia, Universidade Católica Portuguesa, Rua Dr. António Bernardino de Almeida, 4200-072 Porto, Portugal*

Calcium alginate gel beads readily interchange solutes with the bulk solution and water with the surrounding media. The transfer properties are often critical for its use, either for its stability and preservation or textural modulation, or for the convenient treatment of contained tissues for cryopreservation. Chitosan has been evaluated for various uses in food, medical, pharmaceutical, agricultural and chemical industries because of its non-toxic, biocompatible, mucoadhesive, and biodegradable properties. A new approach for chitosan application is analyzed: to both protect against microbial-derived damages and to consider permeability modulation on alginate gel beads employed in cryopreservation. Characterization of combined systems of calcium alginate with chitosan coating should be addressed before including the germplasm tissue. The effect of polysaccharide composition was evaluated on dehydration kinetics. Frozen and unfrozen water fractions for beads with and without chitosan coating were determined by DSC and thermodynamic parameters were calculated. Microstructure was evaluated by SEM, cryo-SEM and FTIR. Results obtained suggest a promising utility of these polysaccharides combination for cryopreservation protocol.

KEYWORDS: *Alginate, Chitosan, Beads, Cryopreservation.*

INTRODUCTION

Cryopreservation offers long-term storage capability, maximal stability of phenotypic and genotypic characteristics of stored germplasm, minimal storage space and maintenance requirements.[1–3] Cryopreservation results in arrested metabolic and biochemical processes, such as cell division and growth.[2, 4] Other biophysical processes leading to protein and nucleic acid degradation would also be halted. Thus, the plant material can be stored without deterioration or modification for unlimited periods,[5] maintaining its genetic stability and regeneration potential.[6–8]

It is usually performed in liquid nitrogen (LN) at −196 °C, and it is the method currently available ensuring the safe, efficient, and cost-effective storage of germplasm of many plant species. Among cryopreservation methods, encapsulation-dehydration is also used because it is applicable to many species,[3, 9] it is based on the successive osmotic and evaporative dehydration of plant cells, previous to the liquid nitrogen (LN) cooling step.[10] Dehydration techniques allow more flexibility when handling large number of samples because the processing is less time-critical than the vitrification techniques *sensu stricto*.[11] Encapsulation-dehydration also avoids the use of toxic cryoprotectants as compared to other methods like droplet-vitrification which employs dimetyl sulfoxide (DMSO).[12]

The concept of synthetic seed was given by Murashige[13] but first report on the development of synthetic seeds was published by Kitto and Janick.[14] They reported the production of desiccated synthetic seeds by coating a mixture of carrot somatic embryo in a water-soluble resin, polyoxyethylene glycol (Polyox). Based on the established technologies, there are two types of synthetic seeds: hydrated and desiccated. Nevertheless, the most studied method involves the encapsulation of propagules in hydrogel for synthetic seed production.[15] A number of coating agents such as sodium alginate, potassium alginate, carrageenan, sodium alginate with gelatin, sodium pectate, carboxymethyl cellulose etc. were used for encapsulation.

*Author to whom correspondence should be addressed.
Email: teixeiraline@hotmail.com
Received: 26 June 2013
Accepted: 11 November 2013

 2328-7519/2014/2/046/009 doi:10.1166/jcc.2014.1039

Among these substances sodium alginate has been extensively used because its many advantages like, easily dissolution and high stability at room temperature.[16–18]

Calcium alginate gel beads are increasingly used for many applications, due to their versatility, inert and non-toxic properties. Alginate is an anionic linear polysaccharide containing 1,4-linked D-mannuronic acid and L-guluronic acid residues, which can form hydrogels in the presence of some multivalent metal ions such a calcium.[19] Alginate is a natural sea-origin product produced by brown sea algae. The gelling behavior of alginate can be exploited for generating spheres, simply by dispersing droplets of sodium alginate in a calcium solution. Beads of different sizes and consistencies can be produced to carry a variety of contents, from food additives and pharmaceuticals, to small objects, such as plant embryos or other tissues for tissue culture purposes.[20–22]

Chitosan is a linear polyaminosaccharide derived from chitin, the principal component of protective cuticles of crustaceans, by *N*-deacetylation and consequently exhibits a large number of amino groups. Chitosan has proved to have a wide range of interesting properties, among others, antimicrobial, protective, antioxidant, plant defense promoting and ligand binding.[23] Being a cationic polysaccharide, it can externally bind to alginate beads or diffuse into the three-dimensional alginate gel network, of anionic character. The combined use of alginate beads with chitosan has been successfully tested on several fields.[24]

The mechanisms underlying the effects of chitosan against plant disease are little known, but would include direct microbial toxicity and metal chelation, as well as the formation of physical barriers. Additionally, it would trigger signalling cascades leading to defence activation. The plant defence enhancing properties of chitosan include the induction of lignification, pH cytoplasm changes, chitinase activation, reactive oxygen species scavenging and other biochemical and genetic responses.[25–27] Chitosan has a role in early elicitation of plant defence,[28] promoting the accumulation of its related metabolites. A possible way of action is the recognition of chitosan, among other cell wall polysaccharides, by specific intruder receptors.[29]

Chitosan has been used to promote the germination of plants of several species, such as maize, peanut or rice.[30–32] Additionally, it promotes wound healing by means of its binding properties[33] and its applicability to fresh product storage is promising. Chitosan also has been reported to have an interesting antioxidant activity,[34–36] and it can function as an oxidative molecule scavenger.

The main drawbacks of calcium alginate gel beads for cryopreservation purpose, is their macroporous structure which could facilitate the interchange of solutes with the external medium. The transfer properties are often critical for its use, either for its stability and preservation or textural modulation, or for the convenient treatment of contained tissues for cryopreservation. The application of chitosan will form a membrane on polyanionic alginate beads due to charge interactions, and by displacing calcium and forming chitosan-alginate crosslinks.[37] This external chitosan layer could decrease porosity, improving the permeability of the system with the extra benefit of showing antimicrobial activity in the capsule surface. In these cases, the antimicrobial protection conferred by chitosan can be also of great interest, as often cultivation and growth after cryopreservation can be impaired by microbial contamination. Microbial proliferation is often a surface affair and gel beds can constitute a suitable model for the study of the interface microbial growth. With the purpose of studying the possible application of chitosan to improve the performance of the encapsulating substrates employed, the permeability and water interaction properties of chitosan-covered alginate beads were investigated. Additionally, FT-IR analyses and scanning electron microscopic techniques were applied to observe microstructure and the chitosan layer on the beads.

MATERIALS AND METHODS

Chitosan Types and Hydrodynamic Characterization

Three different chitosan commercial forms were obtained from Sigma Aldrich (USA): *chitosan C* (from shrimp shells, Sigma No. C3646), *medium molecular weight chitosan* (MMW) (Sigma No. 448877) and *low molecular weight chitosan* (LMW) (Sigma No. 448869). The producer specifications indicated that all of them were 75–85% deacetylated and had been extracted from crustaceous shells. All samples were prepared at a concentration of 3.0 mg/mL dissolved in 0.2 M acetate buffer pH 4.3.

Sedimentation velocity determinations were performed with chitosan dilutions using an Optima XL-I analytical ultracentrifuge (Beckman Instruments, Palo Alto, USA). Samples were centrifuged at 45000 rpm, at a temperature of 20.0 °C. Data were analyzed using the least-squares $c(s)$ method included in the SEDFIT software.[38] Sedimentation coefficients, **s**, were extrapolated to zero concentration, to correct for non-ideality effects.[39]

The sedimentation coefficient—molecular weight power-law relation[40,41] was applied to calculate approximate molecular weights for chitosan, from the determined sedimentation coefficients, using the Eq. (1):

$$\mathbf{s}^{\circ}_{\mathbf{20,W}} = \kappa_{\mathbf{s}}\mathbf{M}^{\mathbf{b}} \qquad (1)$$

where **M** is the molecular weight and $\mathbf{s}^{\circ}_{\mathbf{20,W}}$, the sedimentation coefficient at infinite dilution and normalised to the density and viscosity of water at 20 °C.[40] The pre-exponential factor $\kappa_{\mathbf{s}}^{40}$ a constant for a particular polymer under a defined set of conditions (not to be confused with $\mathbf{k}_{\mathbf{s}}$), and the exponent **b**, defining the hydrodynamic behavior (ranging from 0.4–0.5 for a coil, ~0.15–0.2 for a rod and ~0.67 for a sphere). Values of $\mathbf{k}_{\mathbf{s}} = 0.1$ and $\mathbf{b} = 0.24$ were adopted from data fitted for chitosan samples of similar acetylation degree.[41]

Alginate Beads

Calcium alginate beads were made with 2 or 3% (w/v) low viscosity alginic acid (Sigma, USA) in liquid Murashige and Skoog medium (MS)[42] without calcium, at pH 5.7. Droplets of sodium alginate were pipetted onto 100 mM calcium chloride ($CaCl_2$) solution, using a 2 ml plastic disposable Pasteur pipette, in a flow chamber, at room temperature. Beads were allowed to stand in the $CaCl_2$ solution for 30 min. Then, this solution was filtered to remove the formed calcium alginate beads.

Chitosan Solution and Alginate Bead Treatment

2% C type chitosan solutions were prepared in 1% acetic acid (Protanal, Norway), diluted in MilliQ water (Millipore, Billerica, USA) and stirred overnight. pH was adjusted to 5.6 with NaOH.[43] Calcium alginate beads were stirred at 150 rpm, for 30 min in the selected chitosan solution. Then, chitosan-coated beads were filtered to recover the beads from chitosan solution.

Water Content Determination and Air Dehydration Studies

Four sets of three beads were used for determining the dry mater and water content. Dry matter resulted from differential weighing before and after oven-drying (~85 °C, 72 h) and was expressed as relative to the total mass (**dm**). The water content of beads ($\mathbf{W}_c$) was calculated by difference and it was expressed as relative to the total sample mass-fresh weight-($\mathbf{W}_{c(\mathrm{rel})}$).

To study the beads air-dehydration kinetics, freshly made beads were transferred to an open glass Petri dish and dehydrated for 1, 2, 3, 4, 5 and 6 h in a laminar-flow hood. Afterwards, bead weight was determined and parameters were calculated as described above.

Differential Scanning Calorimetry and Determination of Frozen and Unfrozen Water Fractions

DSC experiments were performed with a Mettler-Toledo DSC 30 instrument (Mettler-Toledo, Griefsen, Switzerland). Three beads were placed in a DSC pan, which was sealed and weighed. Samples were submitted to a cooling scan from room temperature to −150 °C, equilibrated for 5 min at this temperature, followed by a warming scan (at 10 °C min^{-1}), back to room temperature. Calorimetric data were collected from two replicates per treatment. Later, pans were punctured and dried in an oven at 85 °C, for 72 hours, when they showed constant weigh.

Thermograms were analyzed using the standard procedures provided in the Mettler-Toledo STARe software. Freezing temperature (T_f) was determined from the ice thawing thermal events, more precise than freezing ones. The routine produced the onset temperature, $T_{f(\mathrm{onset})}$, corresponding to the equilibrium freezing temperature and that of the peak, $T_{f(\mathrm{peak})}$. The melting enthalpy ΔH_f, proportional to the area of the peak was also obtained. It was expressed as relative to either the total beads mass ($\Delta H_{f(\mathrm{rel})}$), its dry mass ($\Delta H_{f(\mathrm{dm})}$) or its water content $\Delta H_{f(w)}$, to allow easier data comparison. Water fractions, frozen water (W_f) and unfrozen water (W_u), were calculated by comparison between ΔH_f and the pure water freezing enthalpy ($\Delta H_{f(w)} = 333.4$ J/g at 0 °C), together with the total water content previously determined, after Eq. (2):

$$\mathbf{W}_f = (\Delta \mathbf{H}_f / \Delta \mathbf{H}_{f(w)}); \quad \mathbf{W}_u = \mathbf{W}_c - \mathbf{W}_f \qquad (2)$$

Specific enthalpy values (per sample gram) were always used, after the corresponding oven dry pan weighs. Frozen ($\mathbf{W}_f$) and unfrozen ($\mathbf{W}_u$) water contents were expressed as relative to the total bead mass ($\mathbf{W}_{f(\mathrm{rel})}$, $\mathbf{W}_{u(\mathrm{rel})}$), its dry mass ($\mathbf{W}_{f(\mathrm{dm})}$,$\mathbf{W}_{u(\mathrm{dm})}$) or its total water content ($\mathbf{W}_{f(w)}$, $\mathbf{W}_{u(w)}$).

Fourier Transform Infrared Spectrometry (FT-IR)

The employed equipment was a Nicolet 380 FT-IR (USA). Disks were obtained by milling 5 mg of sample with 100 mg of KBr and were analyzed by transmission taking 64 scans per experiment with a resolution of 4 cm^{-1}. Analysis was performed on the following samples: pure materials, capsules with and without chitosan layer.

Low Temperature Scanning Electron Microscopy Observations

Cryo-SEM studies were performed, as previously described,[44] using a Zeiss DSN 960 scanning microscope equipped with a Cryotrans CT-1500 cold plate (Oxford, UK). Cryo-SEM allows sample observations without the need of prior chemical fixing or drying processes. Three beads were fitted on a special bracket and this piece was immersed into liquid nitrogen (LN) for microscopic observation. The holder with the samples was placed in the microscope and etching (partial ice sublimation, induced to provide contrast) was performed for three minutes at −90 °C. Afterwards, the samples were coated with high purity Au, which acts as a conductive contact for electrical charge. Finally, they were inserted in the Cryotrans cold plate and observed under secondary electron mode, at a temperature of −150/−160 °C, using an accelerating voltage of 15 kV and a working distance of 10–25 mm.

Environmental Scanning Electron Microscopy

Environmental SEM analysis was performed using a Jeol JSM-6360 (Japan) microscope. Beads were attached to stubs using a two-sided adhesive tape, then coated with a layer of gold (40 nm–50 nm) and examined using an acceleration voltage of 10 kV. The observation temperature was 5–8 °C and the pressure at the sample chamber was 6 torr. Some beads were air dehydrated for five hours before observation.

Statistical Analysis

Data analysis was performed with the software SYSTAT INC. (Evenston, USA). Analysis of variance (ANOVA) and mean comparisons were carried out. Unless indicated, a level of 95% of confidence ($\alpha = 0.05$) was used. *T*-tests were also performed.

RESULTS AND DISCUSSION

Chitosan Hydrodynamic Characterization

The sedimentation coefficients for each chitosan type were determined and the inverse values were represented as a function of the concentration (Fig. 1), to obtain the infinite dilution extrapolated sedimentation coefficients, $\mathbf{s^{\circ}_{20,w}}$, which are shown in Table I. The molecular weights calculated using the extended Fujita approach, as described (Eq. (1)), are also presented in Table I. The most common commercially available chitosan presentations are often highly polydisperse and their molecular weight can present large differences among batches. Employing this relatively easy approach, the size of the chitosan polymers studied were also estimated (Table I), with the help of fitting parameters obtained for similar samples.[40]

The sedimentation coefficient concentration dependence factor, $\mathbf{k_s}$, accounts for non-ideality, i.e., interparticle interactions.[45] This effect arises from the increased viscosity of the solution at higher concentrations, and from the fact that sedimenting solute particles must displace solvent backwards in the process. Both effects become vanishingly small as concentration decreases. It contains information on the particle size, shape and conformation, as well as on their degree of intermolecular interactions. $\mathbf{k_s}$ is small for globular particles, but becomes much larger for elongated molecules.[46] It is calculated from the slope of the plots in Figure 1 and it is also shown in Table I. The data obtained for sedimentation coefficients and molecular weight of chitosans is of a similar order to those reported, for samples of different origin.[41,45,47] These authors found that data treatment derived from semi-flexible elongated particles fitted well the experimental determinations from chitosan. At the experimental conditions at which these experiments were performed (pH 4.3), the ionisable groups of chitosan would be positively charged and, depending on the extent of charge shielding, the repelling charges would help keep the molecule in a more elongated conformation.

From the molecular weights, the number of monomers obtained for each chitosan type is also showed on Table I. Taking as monomer weights 221 for *N*-acetyl glucosamine (the acetylated monomer) and 179 for glucosamine (the deacetylated subunit), a pondered average monomer weight of 187 can be considered, for chitosans of this deacetylation degree (approximately 80%).

Although further information would be required to calculate a flexibility degree or a persistence length, the simple contour length (not so different here from the length of the extended chain) can be calculated with a mass per unit length value of 420 g mol^{-1} nm^{-1}.[39,42] Results show that chitosan molecules are quite large, almost macroscopic (approximately 1 μm).

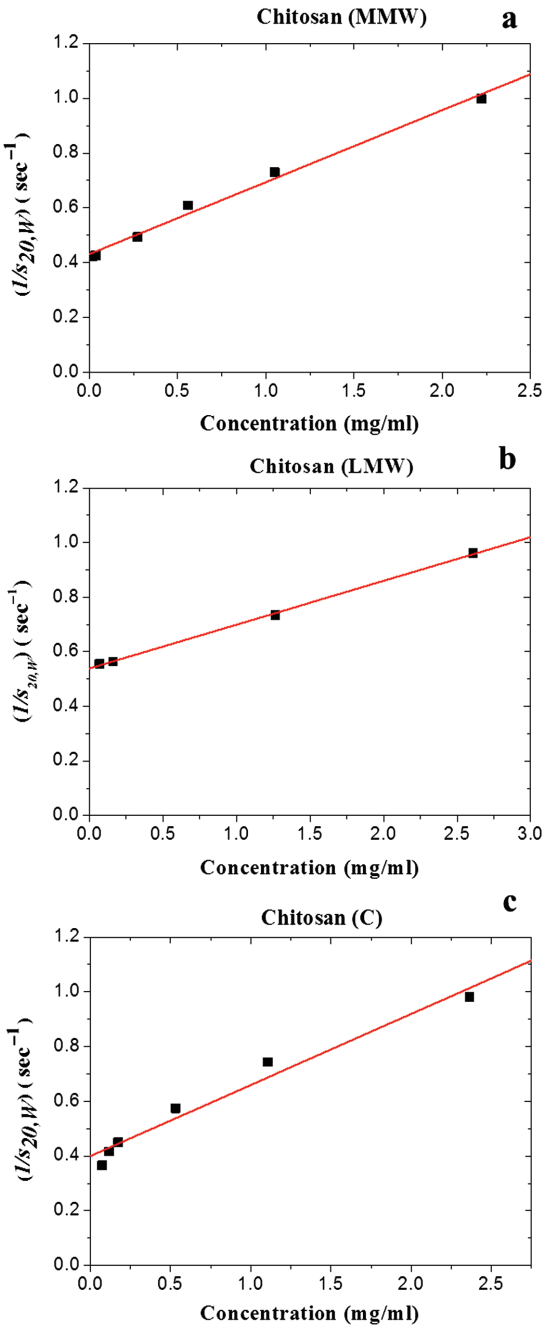

Figure 1. Plots for extrapolation of the sedimentation coefficient of the different chitosan types to infinite dilution: (a) = MMW, (b) = LMW and (c) = C chitosan.

In spite the lack of clear understanding of the mechanisms by which chitosan produces its different effects and activities, such as antimicrobial, antioxidant, plant defence responses eliciting,[23,49] references to the size-dependence are frequent. Most reports ascribe a more pronounced effect to larger size chitosan molecules, for the same

Table I. Analytical ultracentrifugation-derived and chitosan size parameters.

Type of chitosan	$s^{\circ}_{20,w}$ (s)	k_s (mL·g^{-1})	M ($\times 10^3$)	N° monomers	Length (nm)
Chitosan (MMW)	2.32 ± 0.07	608 ± 35	490 ± 50	2600 ± 300	1200 ± 700
Chitosan (LMW)	1.85 ± 0.02	297 ± 7	190 ± 8	1020 ± 40	450 ± 20
Chitosan (C)	2.50 ± 0.20	650 ± 72	670 ± 200	3580 ± 1000	1600 ± 500

acetylation degree.[23,50] However, some others report activities, such as chitosan plant antiviral action, that seem to be inversely correlated to molecular weight.[51] However, most of these differences are among low condensation-degree oligomers, rather than referring to chains as large as those compared here.[50,52] Although the size differences among the three chitosan types employed are not too extreme, the higher molecular mass type ("C") was chosen to perform further experiments. Besides, C chitosan is a cheaper product with extensive use.

Water Content Determination and Air Dehydration

Table II shows relative dry mass (**dm**) and water content of 2 or 3% calcium alginate beads, naked (AB) or covered by chitosan (ACB). Water content was expressed relative to total mass ($\mathbf{W}_{c(\mathrm{rel})}$). Both dry matter and water contents showed little differences between AB and ACB.

The evolution of the water content for 2 and 3% calcium alginate AB and ACB, upon air flow dehydration with time is presented in Figure 2. $\mathbf{W}_{c(\mathrm{rel})}$ was chosen for representation because this value has no dependence with the water content allowing comparison on the same basis. The dehydration behaviour was similar for all bead types except for 2% alginate beads, whose water content decay was slower during the first hour. The plateau where most water has been eliminated was reached between 2 and 3 hours drying time. The layer of chitosan on the beads surface had no significant effect on water content or on drying rate ($p > 0.05$). However, from Figure 2, the presence of a chitosan layer seems to show a modulating effect on drying, regardless of calcium alginate bead concentration. Statistical analysis confirmed that bead formulation was a significant factor before 3 hours: AB (3% alginate), ACB (2% alginate) and ACB (3% alginate) showed the same behaviour along dehydration time, whereas AB (2% alginate) needed extra time to reach the same water content than the other formulations. At longer times no significant differences were found between formulations.

Table II. Water and dry matter content for alginate beads (AB) and chitosan-covered alginate beads (ACB).

	AB		ACB	
	2% alginate	3% alginate	2% alginate	3% alginate
dm ($g_{dm}\ g^{-1}_{sample}$)	0.03 ± 0.01	0.05 ± 0.01	0.04 ± 0.01	0.03 ± 0.01
$W_{c(rel)}$ ($g_{water}\ g^{-1}_{sample}$)	0.97 ± 0.03	0.95 ± 0.03	0.96 ± 0.03	0.97 ± 0.01

Note: See Materials and Methods for parameter description.

Calorimetric Studies on Water Status

Calorimetric measurements designed to obtain information on the water status on beads were performed for 3% alginate beads (AB and ACB). Calorimetric parameters corresponding to the fully hydrated beads are shown in Table III, again little differences between bead types were detected. Melting temperatures were found to be similar ($p > 0.05$). The melting enthalpy obtained, which allowed the calculation of water frozen and unfrozen fractions, was different for both bead types ($p < 0.05$). The slightly higher unfrozen water content of ACB may reflect the intake of an additional water amount on the chitosan covering step, but the presence of this water content after equilibration would imply additional interactions with the electrostatically charged chitosan. This could mean that this additional water amount would not be frozen when temperature was reduced, which is not sustained by these observations. Alternatively, the slightly higher frozen water content of ACB may be due to a lower amount of water interacting with alginate, resulting from a saturation of the alginate charged groups by the chitosan-alginate electrostatic interaction. However, only in $\mathbf{W}_{f(\mathrm{rel})}$ significant differences were found between type of beads.

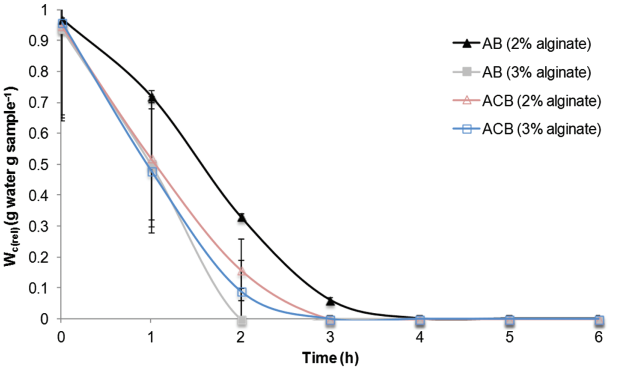

Figure 2. Evolution of the water content over total sample mass, $\mathbf{W}_{c(\mathrm{rel})}$, with air flow drying time, for alginate beads with and without chitosan, prepared with 2 and 3% sodium alginate concentration.

Table III. Calorimetric parameters (mean ± standard deviation) obtained for 3% alginate beads (AB) and chitosan-covered alginate beads (ACB).

	AB	ACB
$T_{f(onset)}$ (°C)	−5.1 ± 0.1	−4.5 ± 0.1
$T_{f(peak)}$ (°C)	4.9 ± 1	5.8 ± 0.2
$\Delta H_{f(rel)}$ (J g_{sample}^{-1})	255 ± 2	277 ± 2
$\Delta H_{f(w)}$ (J g_{w}^{-1})	284 ± 5	296 ± 7
$W_{f(rel)}$ (g_{water} g_{sample}^{-1})	0.76 ± 0.02	0.85 ± 0.1
$W_{f(dm)}$ (g_{water} g_{dm}^{-1})	7.5 ± 0.8	12.9 ± 2.6
$W_{f(w)}$ (g_{water} g_{water}^{-1})	0.85 ± 0.01	0.89 ± 0.02
$W_{u(rel)}$ (g_{water} g_{sample}^{-1})	0.13 ± 0.1	0.11 ± 0.02
$W_{u(dm)}$ (g_{water} g_{dm}^{-1})	1.3 ± 0.3	1.7 ± 0.6
$W_{u(w)}$ (g_{water} g_{water}^{-1})	0.15 ± 0.1	0.11 ± 0.02

Note: See Materials and Methods for parameter description.

Fourier Transform Infrared Spectrometry (FT-IR)

When control beads of calcium alginate were formed, the sodium alginate O—H stretching band at ≈3380 cm^{-1} shifted to 3430 cm^{-1} (Fig. 3). By comparing absorbance spectra, it could be observed that this band grew in intensity. In contrast, the O—H shoulder at 3250 cm^{-1} did not appear to be modified. The modification of the 3380 cm^{-1} band was attributed to intramolecular bonding, whereas the shoulder at 3250 cm^{-1} was related to intermolecular binding.[53]

In the chitosan beads (ACB), the 3430 cm^{-1} band became a little broader. This effect could be associated to a contribution of the pure chitosan, in which the O—H and N—H stretching bands overlapped in the 3600–3000 cm^{-1} region.[54]

The sodium alginate COO-peaks at ≈1610 and 1415 cm^{-1} (asymmetric and symmetric stretch, respectively) became broader in all the capsules and exhibited a large shift to high wavenumbers (from 1415 to 1422 cm^{-1}). As this was a specific ion binding peak, when calcium ions replace sodium ions in the alginate blocks, a new environment around the carbonyl group was created.[53] Since calcium alginate beads have free carboxylic groups, interaction with the amino groups of the chitosan molecule was highly expected. Accordingly, when chitosan was present in the capsules, important changes appeared in the spectra. Smitha, Sridhar, and Khan[55] assigned the shoulder observed at about 1640 cm^{-1} to a symmetric $-NH_3C$ deformation. The shoulder at 1560 cm^{-1} could be assigned to the sum of two effects: chitosan Amide II band and the interaction between alginate and the amino group of the chitosan.

A shoulder is also observed at 1440 cm^{-1} with a decrease in the 1422 cm^{-1} band. This effect could be attributed to the replacement of some Ca^{+2} ions for amino groups of the chitosan around the carbonyl group. The bands observed at 1035 and 950 cm^{-1} assigned to sodium alginate C—O stretching, shift to 1031 and 945 cm^{-1} in the calcium alginate beads and to 1029 and 944 cm^{-1} in the chitosan-coated beads.

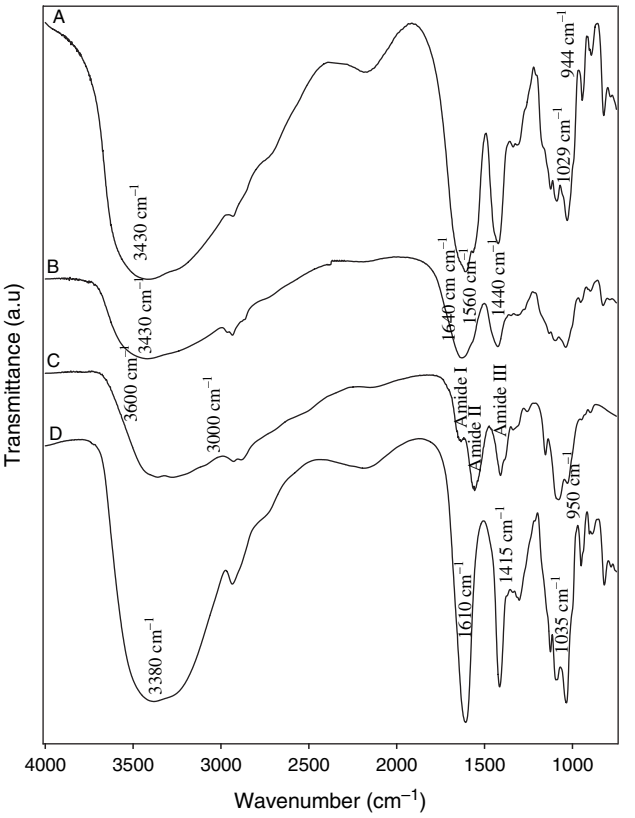

Figure 3. FT-IR spectra in the 4000–900 cm^{-1} region of (A) calcium alginate beads, (B) chitosan coated alginate beads, (C) chitosan and (D) sodium alginate.

Scanning Electron Microscopy of Alginate Beads With and Without Chitosan

Figure 4 shows the aspect of the external surface of AB and ACB under cryo-SEM. As the purpose of the experiment was to examine the external bead surface under liquid nitrogen temperature, etching was not performed. No evident differences could be appreciated in bead examination: chitosan would form a homogeneously distributed film, completely covering the surface of alginate beads, and the aspect of both AB and ACB would be similar. There were no evident changes, such as patches or cracks, on the chitosan layer, although cooling to liquid nitrogen temperature was performed by quenching, a process that could induce mechanical stress on the bead surface.

Figure 5 compares the surfaces of AB and ACB, as observed under an environmental scanning electron microscope, i.e., at room temperature and reduced pressure. Again, the surface aspect of both bead types was not especially different for non-dehydrated beads. Nevertheless, beads after an advanced dehydration time (5 hours) showed a wrinkled surface in ACB, probably resulting from the chitosan layer adaptation to the bead reduced volume after drying.

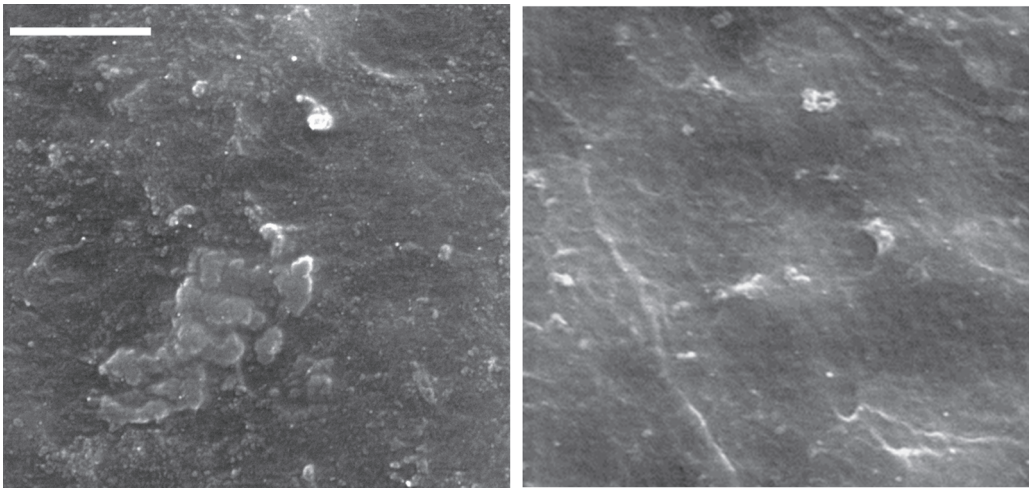

Figure 4. **Cyro-SEM micrographs showing the external AB (right) and ACB (left) bead surface after quench cooling to liquid nitrogen temperature. The bar corresponds to 5 μm.**

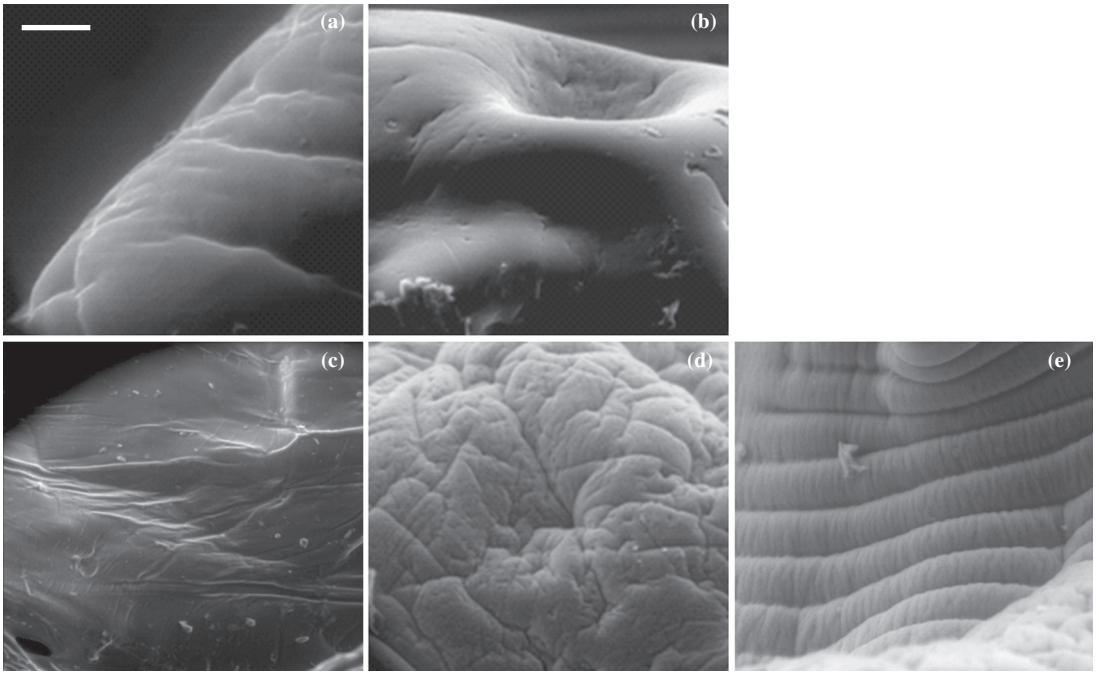

Figure 5. **Environmental SEM micrographs showing bead surfaces after different air-flow dehydration times: (a) AB and (c) ACB (0 hours-not dehydrated beads); (b) AB, (d) and (e) ACB (5 hours dehydration). The bar corresponds to 50 μm for (a) and (e) and to 100 μm for (b)–(d).**

DISCUSSION

The transfer properties of alginate beads would be critical for its use, either for its stability and gel integrity, or for the convenient treatment of contained tissues for cryopreservation. The addition of an external layer of chitosan would have an influence on the matter transfer properties of AB. Chitosan has been applied, for example, to modulate plant water interchanges and transpiration, by creation of an anti-transpirant film.[56, 57] However, in the formulation employed here, there were not important changes when the chitosan layer has been added to alginate beads with respect to water interaction behaviour, water initial retention and water loss after four hours air-flow dehydration, although the interaction between alginate and chitosan forming an external layer was evidenced by FT-IR analysis. Small changes could be observed in water freezing behaviour; however the impact of this difference in sample parameters need to be checked in germplasm cryopreserved assays.

The alginate beads employed in this study behave quite differently from the beads actually employed in cryopreservation practice. In the traditional

encapsulation-dehydration protocol[58] the alginate beads had been cultured in 0.75 M sucrose. Meanwhile, the beads in this work had a much lower solute concentration, only that corresponding to the salts and other nutrients of MS medium, with a total ionic strength of 94.25 mM.[42, 59] For example, the traditional protocol uses 6 hours drying to reach constant water content, in contrast to coated beads only needed 4 hours.

In other works, a three-dimensional network made from chitosan and alginate have been utilized, for example as prospective tissue engineering scaffolds.[60] However, the process followed here caused chitosan to form an external layer around alginate beads. The chitosan layer of ACB beads behaved well towards liquid nitrogen cooling, not showing any sign of cracking or other type of alteration when inspected by cryo-SEM. However, environmental SEM revealed that the chitosan external layer gets wrinkled, in association to the changes in water content and bead volume caused by dehydration. A stripped or wrinkled bead surface was reported also by Anbinder et al.[24] when observing ACB.

CONCLUSION

The results obtained in this work encourage the applicability of chitosan to the alginate beads employed in cryopreservation, since the most important gel properties, such as its water interaction behaviour, were found to be scarcely altered. Besides, the antimicrobial protection conferred by chitosan and their antioxidant properties can be also of great interests, as often cultivation and growth after cryopreservation can be impaired by microbial contamination or cellular oxidative damages.

Acknowledgments: Work carried out thanks to project "CRYODYMINT" (AGL2010-21989-C02-02), Spanish Science and Innovation Ministry. A. S. Teixeira was supported by CSIC, via the JAE-Pre program, partially funded from ESF. C. F. Fernandes was supported by ERASMUS Program 2011/2012—Mobility Students/Professional Internships, partially funded from European Social Fund (ESF) associated with Universidade Católica Portuguesa-Porto, Portugal. Assistance provided by Professor S. E. Harding and Gary Adams and Dr. Fahad Almutairi, from the National Centre for Macromolecular Hydrodynamics, School of Biosciences, University of Nottingham, England, is gratefully acknowledged.

REFERENCES

1. F. Engelmann, *In vitro* germplasm conservation methods. *Acta Hortic.* 461, 41 **(1997)**.
2. F. Engelmann, Importance of cryopreservation for the conservation of plant genetic resources, Cryopreservation of Tropical Plant Germplasm, edited by F. Engelmann and H. Takagi, International Plant Genetic Resources Institute, Rome **(2008)**, pp. 8–20.
3. R. A. Shibli, Cryopreservation of black iris (*Iris nigricans*) somatic embryos by encapsulation-dehydration. *Cryo Letters* 21, 39 **(2000)**.
4. L. E. Towill, Vitrification as a method to cryopreserve shoot tips, Plant Tissue Culture Concepts and Laboratory Exercises, edited by R. S. Trigiano and D. J. Gray, CRC Press, Boca Raton **(1996)**, pp. 297–304.
5. S. E. Ashmore and F. Engelmann, Status Report on the Development and Application of *In Vitro* Techniques for the Conservation and Use of Plant Genetic Resources, International Plant Genetic Resources Institute, Rome **(1997)**.
6. K. Rajasekaran, Regeneration of plants from cryopreserved embryogenic cell suspension and callus cultures of cotton (*Gossypium hirsutum L.*). *Plant Cell Rep.* 15, 859 **(1996)**.
7. T. Matsumoto, A. Saki, and Y. Nako, A novel preculturing for enhancing the survival of *in vitro*-grown meristems of wasabi (*Wasabia japonica)* cooled to −196 °C by vitrification. *Cryo Letters* 19, 27 **(1998)**.
8. L. E. Towill, Cryopreservation of *Mentha* (mint), Cryopreservation of Plant Germplasm II, edited by L. E. Towill, Springer, Heidelberg **(2002)**, pp. 151–163.
9. P. S. Rao, P. Suprasanna, T. R. Ganapathi, and V. A. Bapat, Synthetic seeds: Concepts, methods and application, Plant Tissue Culture and Molecular Biology, edited by P. V. Srivastava, Narosa, India **(1998)**, pp. 607–19.
10. T. W. Swan, D. O'Hare, R. A. Gill, and P. T. Lynch, Influence of preculture conditions on the post-thaw recovery of suspension cultures of Jerusalem artichoke (*Helianthus tuberosus L.*). *Cryo Letters* 20, 325 **(1999)**.
11. A. Sakai, T. Matsumoto, D. Hirai, and T. Niino, Newly developed encapsulation-dehydration protocol for plant cryopreservation. *Cryo Letters* 21, 53 **(2000)**.
12. R. A. Shibli, M. A. Shatnawi, W. S. Subaih, and M. M. Ajlouni, *In vitro* conservation and cryopreservation of plant genetic resources: A review. *WJAS* 2, 372 **(2006)**.
13. T. Murashige, Plant cell and organ cultures as horticultural practices. *Acta Hortic.* 78, 17 **(1977)**.
14. S. L. Kitto and J. Janick, Polyox as anartificial seed coat for a sexual embryos. *Hortic. Sci.* 17, 448 **(1982)**.
15. K. Redenbaugh and K. Walker, Role of artificial seeds in alfalfa breeding, Plant Tissue Culture: Applications and Limitations, edited by S. S. Bhojwani, Elsevier, Amsterdam **(1990)**, pp. 102–35.
16. K. Redenbaugh, J. A. A. Fujii, and D. Slade, Hydrated coatings for synthetic seeds, Synseed—Applications of Synthetic Seeds to Crop Improvement, edited by K. Redenbaugh, CRC Press, Boca Raton, Florida **(1993)**, pp. 35–46.
17. H. Ara, U. Jaiswal, and V. S. Jaiswal, Synthetic seed: Prospects and limitations. *Curr. Sci.* 78, 1438 **(2000)**.
18. M. K. Rai, P. Asthana, S. K. Singh, V. S. Jaiswal, and U. Jaiswal, The encapsulation technology in fruit plant-a review, *Biotech. Adv.* 27, 671 **(2009)**.
19. T. Coviello, P. Matricardi, C. Marianecci, and F. Alhaique, Polysaccharide hydrogels for modified release formulations. *J. Controlled Release* 119, 5 **(2007)**.
20. F. Engelmann, M. T. G. Arnao, Y. Wu, and R. Escobar, The development of encapsulation dehydration, Plant Cryopreservation: A Practical Guide, edited by B. M. Reed, Springer, New York **(2008)**.
21. M. Phunchindawan, K. Hirata, A. Sakai, and K. Miyamoto, Cryopreservation of encapsulated shoot primordia induced in horseradish (*Armoracia rusticana)* hairy root cultures. *Plant Cell Rep.* 16, 469. **(1997)**.
22. M. K. Rai, P. Asthana, S. K. Singh, and V. S. Jaiswal, The encapsulation technology in fruit plants-A review. *Biotechnol. Adv.* 27, 671 **(2009)**.
23. A. El Hadrami, L. R. Adam, I. El Hadrami, and F. Daayf, Chitosan in plant protection. *Mar. Drugs* 89, 68 **(2010)**.
24. P. S. Anbinder, L. Deladino, A. S. Navarro, J. I. Amalvy, and M. N. Martino, Yerba mate extract encapsulation with alginate and chitosan systems: Interactions between active compound encapsulation polymers. *J. Encapsulation Adsorpt. Sci.* 1, 80 **(2011)**.

25. M. S. Barber, R. E. Bertram, and J. P. Ride, Chitin oligosaccharides elicit lignification in wounded wheat leaves. *Physiol. Mol. Plant Pat.* 34, 3 **(1989)**.

26. K. Kuchitsu, H. Kosaka, T. Shiga, and N. Shibuya, EPR evidence for generation of hydroxyl radical triggered by *N*-acetylchitooligosaccharide elicitor and a protein phosphatase inhibitor in suspension-cultured rice cells. *Protoplasma* 188, 138 **(1995)**.

27. E. Minami, K. Kuchitsu, D. Y. He, H. Kouchi, N. Midoh, Y. Ohtsuki, and N. Shibuya, Two novel genes rapidly and transiently activated in suspension-cultured rice cells by treatment with *N*-acetylchitoheptaose, a biotic elicitor for phytoalexin production. *Plant Cell Physiol.* 37, 563 **(1996)**.

28. B. E. Amborabé, J. Bonmort, P. Fleurat-Lessard, and G. Roblin, Early events induced by chitosan on plant cells. *J. Exp. Bot.* 59, 2317 **(2008)**.

29. J. L. Dangl and J. D. G. Jones, Plant pathogens and integrated defence responses to infection. *Nature* 411, 826 **(2001)**.

30. M. V. Reddy, J. Arul, P. Angers, and L. Couture, Chitosan treatment of wheat seeds induces resistance to *Fusarium graminearun* and improves seed quality. *J. Agri. Food Chem.* 47, 1208 **(1999)**.

31. S. L. Ruan and Q. Z. Xue, Effects of chitosan coating on seed germination and salt-tolerance of seedlings in hybrid rice (*Oryza sativa L.*). *Acta Agro. Sin.* 28, 803 **(2002)**.

32. Y. G. Zhou, Y. D. Yang, Y. G. Qi, Z. M. Zhang, X. J. Wang, and X. J. Hu, Effects of chitosan on some physiological activity in germinating seed of peanut. *J. Pean Sci.* 31, 22 **(2002)**.

33. S. Hirano, T. Nakahira, M. Nakagawa, and S. K. Kim, The preparation and applications of functional fibres from crab shell chitin. *J. Biotech.* 70, 373 **(1999)**.

34. W. Xie, P. Xu, and Q. Liu, Antioxidant activity of water-soluble chitosan derivatives. *Bioorg. Med. Chem. Lett.* 11, 1699 **(2011)**.

35. T. Sun, D. Zhou, J. Xie, and F. Mao, Preparation of chitosan oligomers and their antioxidant activity. *Chem. Mat. Sci.* 225, 451 **(2006)**.

36. T. Sun, Q. Yao, D. Zhou, and F. Mao, Antioxidant activity of *N*-carboxymethyl chitosan oligosaccharides. *Bioorg. Med. Chem. Lett.* 18, 5774 **(2008)**.

37. A. R. DeGroot and R. J. Neufeld, Encapsulation of urease in alginate beads and protection from chymotrypsin with chitosan membranes. *Enzyme Microb. Tech.* 29, 321 **(2001)**.

38. J. Dam and P. Schuck, Sedimentation velocity analysis of heterogeneous protein-protein interactions: Sedimentation coefficient distributions $c(s)$ and asymptotic boundary profiles from Gilbert–Jenkins theory. *Biophys. J.* 89, 651 **(2005)**.

39. T. R. Patel, S. E. Harding, A. Ebringerova, M. Deszczynski, Z. Hromadkova, A. Togola, B. S. Paulsen, G. A. Morris, and A. J. Rowe, Weak self-association in a carbohydrate system. *Biophys. J.* 93, 741 **(2007)**.

40. S. E. Harding, K. M. Vårum, B. T. Stokke, and O. Smidsrød, Molecular weight determination of polysaccharides. Advances in Carbohydrate Analysis, E. A. White, JAI Press, Birmingham **(1991)**, Vol. 1, pp. 63–144.

41. S. E. Harding, P. Schuck, A. S. Abdelhameed, G. Adams, M. S. Kök, and G. A. Morris, Extended Fujita approach to the molecular weight distribution of polysaccharides and other polymeric systems. *Methods* 54, 136 **(2011)**.

42. T. Murashige and F. Skoog, A revised medium for rapid bioassays with tobacco tissue cultures. *Physiol. Plant.* 15, 473 **(1962)**.

43. D. Sanchéz-Dominguéz, S. Bautista-Baños, and P. C. Ocampo, Efecto del quitosano en el desarrollo y morfologia de *Alternaria alternata* (FR.) Keissl. *Anales de Biologia.* 29, 23 **(2007)**.

44. A. S. Teixeira, M. E. Gonzalez-Benito, and A. D. Molina-García, Glassy state and cryopreservation of mint shoot tips. *Biotechnol. Prog.* 29, 707 **(2013)**.

45. G. A. Morris, J. Castile, A. Smith, G. G. Adams, and S. E. Harding, Macromolecular conformation of chitosan in dilute solution: A new global hydrodynamic approach. *Car. Pol.* 76, 616 **(2009)**.

46. G. Ralston, Introduction to Analytical Centrifugation, Beckman Instruments, Fullerton, California **(1993)**.

47. G. Berth, H. Cölfen, and H. Dautzenberg, Physicochemical and chemical characterisation of chitosan in dilute aqueous solution. *Prog. Colloid. Polym. Sci.* 119, 50 **(2002)**.

48. I. N. M. Vold, Periodate oxidised chitosans: Structure and solution properties, Doctoral Dissertation, Norwegian University of Science and Technology, Trondheim **(2004)**.

49. M. Kong, X. G. Chen, K. Xing, and H. J. Park, Antimicrobial properties of chitosan and mode of action: A state of the art review. *Int. J. Food Microbiol.* 144, 51 **(2010)**.

50. H. K. No, K. S. Lee, I. D. Kim, Park, and S. P. Meyers, Chitosan treatment effects yield, ascorbic acid content, and hardness of soybean sprouts. *J. Food Sci.* 68, 680 **(2003)**.

51. S. N. Kulikov, S. N. Chirkov, A. V. Il'ina, S. A. Lopatin, and V. P. Varlamov, Effect of the molecular weight of chitosan on its antiviral activity in plants. *Appl. Biochem. Microbiol.* 42, 200 **(2006)**.

52. J. C. Cabrera, J. Messiaen, P. Cambier, and P. van Cutsem, Size, acetylation and concentration of chitooligosaccharide elicitors determine the switch from defence involving PAL activation to cell death and water peroxide production in *Arabidopsis* cell suspensions. *Physiol. Plantarum* 127, 44. **(2006)**.

53. C. Sartori, D. S. Finch, B. Ralph, and K. Gilding, Determination of the cation content of alginate thin films by FT-IR spectroscopy. *Polymers* 38, 43 **(1997)**.

54. H. Y. Zhou, X. G. Chen, M. Kong, C. S. Liu, D. S. Cha, and J. F. Kennedy, Effect of molecular weight and degree of chitosan deacetylation on the preparation and characteristics of chitosan thermosensitive hydrogel as a delivery system. *Car. Pol.* 73, 265 **(2008)**.

55. B. Smitha, S. Sridhar, and A. A. Khan, Chitosan-sodium alginate polyion complexes as fuell cell membranes. *Eur. Polym. J.* 41, 1859 **(2005)**.

56. M. Bittelli, M. Flury, G. S. Campbell, and E. J. Nichols, Reduction of transpiration through foliar application of chitosan. *Agr. Forest Meteorol.* 107, 167 **(2011)**.

57. M. Iriti, V. Picchi, M. Rossoni, S. Gomarasca, N. Ludwig, M. Garganoand, and F. Faoro, Chitosan antitranspirant activity is due to abscisic acid-dependent stomatal closure. *Environ. Exper. Bot.* 66, 493 **(2009)**.

58. E. E. Uchendu and B. M. Reed, A comparative study of three cryopreservation protocols for effective storage of *in vitro*-grown mint (*Mentha* spp.). *Cryo Letters* 29, 181 **(2008)**.

59. B. H. McCown and J. C. Sellmer, General media and vessels suitable for woody plant culture, Cell and Tissue Culture in Forestry, General Principles and Biotechnology, edited by J. M. Bonga and D. Z. Durzan, Martinus Nijhoff Publishers, Dordrecht **(1987)**, pp. 4–16.

60. L. L. Hyland, M. B. Taraban, B. Hammouda, and Y. Y. Bruce, Mutually reinforced multicomponent polysaccharide networks. *Biopol.* 95, 840 **(2011)**.